Comparison of frequency domain measures based on spectral decomposition for spontaneous baroreflex sensitivity assessment after Acute Myocardial Infarction

Riccardo Pernice[a,*,§], Laura Sparacino[a,§], Giandomenico Nollo[b], Salvatore Stivala[a], Alessandro Busacca[a], Luca Faes[a]

[a]Department of Engineering, University of Palermo, 90128 Palermo, Italy
[b]Department of Industrial Engineering, University of Trento, 38123 Trento, Italy
*riccardo.pernice@unipa.it
§These authors contributed equally to this work

Abstract

The **objective** of this study is to present a new method to assess in the frequency domain the directed interactions between the spontaneous variability of systolic arterial pressure (SAP) and heart period (HP) from their linear model representation, and to apply it for studying the baroreflex control of arterial pressure in healthy physiological states and after acute myocardial infarction (AMI). The method is based on pole decomposition of the model transfer function and on the following evaluation of causal measures of coupling and gain from the poles associated to low frequency (0.04-0.15 Hz) oscillatory components. It is compared with traditional non-causal approaches for the spectral analysis of the baroreflex gain, and with causal approaches based on the directed coherence, in a group of AMI patients and in Young and Old healthy controls studied at rest and during head-up tilt. Analysis of feedforward interactions from RR to SAP is also performed. Our **results** support the importance of using local causal approaches to quantify separately baroreflex and feedforward interactions between RR and SAP, allowing both to confirm known physiological behaviors (e.g., weaker baroreflex effectiveness and lower sensitivity after AMI) and to suggest novel findings (e.g., preserved low frequency baroreflex response to postural stress after AMI). We also find that the postural stress alters feedforward interactions selectively across groups, being related to decreased coupling only in Young and to increased gain mostly in AMI. These results have a **significance** for the clinical assessment of the baroreflex and the physiological evaluation of cardiovascular interactions.

1. Introduction

The baroreflex mechanism has a key role in the short-term regulation of systolic arterial pressure (SAP) and heart period (measured as the RR interval of the electrocardiogram, ECG), which are known to dynamically interact in a closed loop, as a consequence of the baroreflex feedback of SAP on RR and of feedforward pathways of mechanical nature, whereby SAP is influenced by previous RR changes [1,2]. The baroreflex represents a fundamental mechanism to maintain the optimal blood pressure level continuously or in response to changing physiological conditions, and accomplishes such a task modulating the heart rate [3–6]. Specifically, a decrease in arterial blood pressure evokes a baroreflex response leading to an increased heart rate, while an increase in arterial blood pressure is followed by the opposite effect. While in healthy subjects the baroreflex acts in response to physiological stressors such as change of posture, mental workload and others, an impairment of the baroreflex control is thought to be often associated with age, orthostatic intolerance and pathologies like heart failure or acute myocardial infarction (AMI), as postural circulatory stress and cardiovascular diseases elicit baroreceptor unloading [7–10]. Therefore, assessment of the baroreflex sensitivity (BRS), often evaluated from the spontaneous beat-to-beat fluctuations of RR and SAP as the magnitude of the reflex change in RR corresponding to a unitary change in SAP (i.e., the so-called baroreflex gain), can provide valuable insight on the cardiovascular regulation in normal and pathological conditions and can have an important diagnostic and clinical value [4,11,12]. An appropriate evaluation of the baroreflex gain should take into account the oscillatory nature of cardiovascular parameters, being able to separate contributions occurring in different frequency bands - typically divided into very low-frequency (VLF, up to 0.04 Hz), low-frequency (LF, 0.04 – 0.15 Hz) and high-frequency (HF, 0.15– 0.4 Hz) bands, as well as the closed-loop nature of cardiovascular interactions [13]. Usually, the frequency analysis of the baroreflex gain is carried out focusing on the LF band to avoid the confounding effects of other variables operating at different frequencies (e.g., respiration), and causal analysis methods are adopted to minimize the effect of non-baroreflex mechanisms on the BRS estimates [14–18]. On the other hand, though much less investigated, the feedforward mechanism from RR to SAP is also important in the assessment of the balanced cardiovascular regulation in normal and diseased conditions [7]. Besides the evaluation of the gain function quantifying the magnitude of the mechanism that links the input to the output time series, measures of coupling and causal coupling such as the spectral coherence and the directed (causal) coherence (DC) are usually computed to assess the strength of cardiovascular interactions. In particular, the DC is a linear frequency domain measure of causal interactions between coupled dynamic processes [11,19] derived from the spectral representation of the vector autoregressive (VAR) model fitting the process dynamics. The DC from a source to a target process is computed exploiting the parametric representation to separate the power spectral density (PSD) of the target process into partial spectra related to its own dynamics and to the dynamics of the source process.

The VAR representation of multiple time series is very popular in the field of cardiovascular variability, where VAR-based measures of coupling and gain such as the DC and the spectral BRS are widely used to characterize cardiovascular interactions in different physiopathological conditions [19–22]. In practical applications, where

both the DC function and the baroreflex gain need to be quantified in specific frequency regions, empirical approaches are generally adopted which consist in taking the maximum or average value, within the band of interest, of the analyzed spectral function. However, these approaches often lead to ambiguous choices (a maximum value can be absent within the observed band) or imprecise quantifications (the average value may be affected by spectral effects of nearby broadband oscillations) [11]. To overcome these limitations, the present study aims at introducing a modification of the causal coherence and of the previous definitions of spectral baroreflex gain [10,23] based on the spectral decomposition method [24]. Specifically, spectral decomposition is applied to the partial spectra of the PSD of the target process, representing each partial spectrum as the sum of bell-shaped functions with features (power, frequency, spectral bandwidth) related to the type and location (modulus and phase) of the poles of the transfer function which defines the vector AR process in the Z-domain. Then, the power content associated to the decomposed spectral components with frequency inside the band of interest (here, the LF band) is elaborated to obtain pole-specific measures of coupling and gain within the band. These measures, which we refer to as "local" due to their frequency-specific nature, are compared in the present work with the corresponding traditional "global" measures obtained as the band-averaged DC and gains.

The proposed local approach for causal spectral decomposition has been first presented in a preliminary form in a conference contribution [25], where it was introduced for the computation of causal coupling and tested in a theoretical example and in representative cardiovascular time series. In this work, the approach is delineated in detail and is extended to the computation of the gain function. Moreover, it is exhaustively tested and systematically compared with global and with non-causal methods on the RR and SAP time series measured in a group of post-AMI patients monitored at rest and during orthostatic stress, as well as in two control groups of healthy subjects (younger and age-matched with AMI). The study group and the experimental protocol are chosen in order to reproduce expected physiological behaviors under which global and local measures of coupling and gain could be compared: the tilt maneuver has been widely demonstrated to stimulate the sympathetic response of the autonomic nervous system and to enhance cardiovascular interactions increasing the coupling between SAP and RR (see e.g. [10,16,26,27]); similarly, it is known that infarction produces impaired autonomic control of the cardiovascular system and attenuated baroreflex activity [7,28]. The comparison of local versus global measures for the causal evaluation of gain and coupling is performed computing the measures along the two directions of interactions of the cardiovascular closed loop and assessing them within the LF band of the frequency spectrum. A main focus of the comparison is the evaluation of the confounding effects of broad-band oscillations which have central frequency outside the LF band but exhibit spectral profiles which enter the LF band; such effects are unavoidably included in the global, band-averaged measures and are instead avoided by the computation of local, pole-specific measures [25].

2. Methods

2.1 Measures of causal coupling and gain derived from parametric cross-spectral analysis

Let us consider a bivariate stochastic process Y composed by two jointly stationary, zero mean discrete stochastic processes y_1 and y_2. Defining $Y(n) = [y_1(n) \ y_2(n)]^T$ as the vector variable sampling the process at time $t_n = nT_s$, where $T_s = 1/f_s$ is the sampling period and f_s the sampling frequency, it is possible to express the causal interactions occurring between the processes in a parametric form through a p-order bivariate autoregressive (AR) model as follows [21,25,29]

$$Y(n) = \sum_{k=0}^{p} A(k)Y(n-k) + U(n) \ , \tag{1}$$

being $U(n) = [u_1(n) \ u_2(n)]^T$ a vector of zero-mean uncorrelated white noises with 2×2 diagonal covariance matrix $\Sigma = \text{diag}\{\sigma_1^2, \sigma_2^2\}$, and $A(k)$ the 2×2 coefficient matrix in which the coefficient $a_{ij}(k)$ describes the interaction from $y_j(n-k)$ to $y_i(n)$ (i,j=1,2). Note that the model (1) is not strictly causal, as it accounts for zero-lag effects through the coefficient matrix $A(0)$, which takes an upper diagonal form with the only non-zero coefficient modeling the effect from $y_2(n)$ to $y_1(n)$ [22]. This model form is set to describe instantaneous interactions between the two processes and guarantee diagonality of the covariance noise matrix Σ.

The estimated model coefficients are represented in the Z domain through the Z-transform of (1), thus yielding $Y(z) = H(z)U(z)$, where the 2×2 transfer matrix is

$$H(z) = \begin{bmatrix} H_{11}(z) & H_{12}(z) \\ H_{21}(z) & H_{22}(z) \end{bmatrix} = [I - A(z)]^{-1} = \bar{A}(z)^{-1} \ , \tag{2}$$

being $A(z) = \sum_{k=1}^{p} A(k)z^{-k}$ the coefficient matrix in the Z domain and I the 2×2 identity matrix. Taking the inverse of $\bar{A}(z)$, each element of the transfer matrix is represented as follows (i,j=1,2)

$$H_{ii}(z) = \frac{\bar{A}_{jj}(z)}{|\bar{A}(z)|}; H_{ij}(z) = \frac{-\bar{A}_{ij}(z)}{|\bar{A}(z)|}. \tag{3}$$

Computing $H(z)$ on the unit circle in the complex plane ($H(f) = H(z)|_{z=e^{j2\pi fT_s}}$), the 2×2 spectral density matrix of the bivariate process in the frequency domain becomes $S(f) = H(f)\Sigma H^*(f)$, where * indicates the Hermitian transpose. In this matrix, the diagonal terms $S_{ii}(f)$ correspond to the auto-spectra, while the off-diagonal terms $S_{ij}(f)$ correspond to the cross-spectra.

From the frequency domain representation of the AR model, the diagonal elements of the spectral density matrix can be elaborated to estimate a non-causal measure of spectral gain from y_j to y_i ($i,j = 1,2, i \neq j$):

$$G_{ij}^{\alpha}(f) \triangleq \sqrt{\frac{S_{ii}(f)}{S_{jj}(f)}} \tag{4}$$

where the superscript α denotes the non-causal index first used by Pagani et al. [23]. The α measure is a non-causal index of gain, because it works under the main assumption that the whole variability of y_i is driven by y_j (i.e., the underlying model is an open loop model without noise such that $S_{ii}(f) = |G_{ij}^{\alpha}(f)|^2 S_{jj}(f)$). To get a causal measure, first each auto-spectrum is expressed as the sum of causal contributions from Eqs. (2, 3) to yield

$$S_i(f) \triangleq S_{ii}(f) = \sigma_i{}^2 |H_{ii}(f)|^2 + \sigma_j{}^2 |H_{ij}(f)|^2 \,, \tag{5}$$

being $\sigma_j{}^2 |H_{ij}(f)|^2 \triangleq S_{i|j}(f)$ the partial spectrum of y_i given y_j (i,j=1,2). A left-side normalization of (5) produces $\gamma_{ii}{}^2(f) + \gamma_{ij}{}^2(f) = 1$, where

$$\gamma_{ij}^2(f) \triangleq \frac{\sigma_j{}^2|H_{ij}(f)|^2}{S_{ii}(f)} = \frac{S_{i|j}(f)}{S_i(f)} \tag{6}$$

is the squared directed (causal) coherence (DC) from y_j to y_i, a function assessing the normalized coupling strength from y_j to y_i in the frequency domain [19]. The DC ranges between 0 and 1, being 0 when y_j does not cause y_i at frequency f, and 1 when the whole power of y_i at frequency f is due to the variability of y_j [29]. The causal information conveyed in the DC allows to define a causal measure of spectral gain, first used by Faes et al. [10]:

$$G_{ij}^{\gamma}(f) \triangleq G_{ij}^{\alpha}(f)|\gamma_{ij}(f)| = \sqrt{\frac{S_{i|j}(f)}{S_{jj}(f)}} = \sqrt{\frac{\sigma_j{}^2|H_{ij}(f)|^2}{S_{jj}(f)}} \tag{7}$$

The γ measure (7) weights the power ratio defined in (4) through the causal coherence from y_j to y_i. In the presence of closed-loop (bidirectional) interactions between y_1 and y_2, this modification allows the causal measure of gain to focus only on the direction of interest, while the non-causal measure tends to mix up influences coming from the two paths of the closed loop [10]. Moreover, since the causal coherence is bounded between 0 and 1, the non-causal measure is always higher than the causal measure, suggesting that the former tends to overestimate the gain.

2.2 Measures of causal coupling and gain derived from causal spectral decomposition

The measures defined by Eqs. (4, 6, 7) are "frequency-specific" in the sense that they are computed at each frequency; therefore, when they have to be computed within a specific frequency band, an "overall" estimate is typically extracted as the average of that measure within the band. For this reason, these are referred to as "global measures" in the following. Nonetheless, such global values in the selected band can be

misleading, being unable to objectively quantify the causal contribution of the source process to the power of the target one [25]. As an alternative, we herein propose "pole-specific" measures that can be related to the poles of the transfer function of the bivariate AR model. Their computation is associated to the pole frequency, and thus allows to get "local" measures of causal coupling or gain, where "local" is meant to indicate individual oscillations localized at specific frequencies. In the following, we define local measures of causal coupling (pole-specific spectral causality, PSSC) and causal and non-causal local measures of gain (pole-specific spectral gain, PSSG) to assess, in the frequency domain, the strength of the coupling of the directed interactions between the two processes and the gain of the transfer functions, respectively.

Exploiting spectral decomposition [24], each transfer function defined as in (3) is decomposed as the sum of q spectral components ($q \cong p/2$), which correspond to the poles of the determinant of $\bar{A}(z)$. Every spectral component is described by a specific profile and has an associated frequency (related to the pole phase) and power (related to the pole residual). In this way, the complex partial PSD of the ith process given the jth process, which can be written in the Z-domain as

$$S_{i|j}(z) = H_{ij}(z)\sigma_j^2 H_{ij}^*(1/z^*), \qquad (8)$$

can be expanded decomposing the $i - j^{th}$ transfer function as

$$H_{ij}(z) = \frac{-\bar{A}_{ij}(z)}{|\bar{A}(z)|} = \frac{-\bar{A}_{ij}(z)}{\prod_k(z-z_k)}, \qquad (9)$$

being the poles z_k, $k=1,...q$ the roots of $|\bar{A}(z)|$. The expansion of each partial spectrum in (8) is performed exploiting the Heaviside decomposition with simple fractions relevant to all its poles (i.e., the poles z_k inside the unit circle and their reciprocals $\bar{z}_k = z_k^{-1}$ outside the unit circle, with $k=1,...,q$), which are fractions weighted by the relevant residuals of $S_{i|j}(z)$ (i.e., $r_k z_k$ and $-r_k \bar{z}_k$), to get [24]

$$S_{i|j}(z) = \sum_{k=1}^q S_{i|j}^{(k)}(z), \ S_{i|j}^{(k)}(z) = \frac{r_k z_k}{z-z_k} - \frac{r_k \bar{z}_k}{z-\bar{z}_k}. \qquad (10)$$

After extracting the residuals and expanding the partial spectrum in simple fractions and given that $S_i(z) = S_{i|i}(z) + S_{i|j}(z)$, we obtain the spectrum of y_i computing (10) for values of z on the unit circle of the complex plane [25]:

$$S_i(f) = \sum_{k=1}^q S_i^{(k)}(f) = \sum_{k=1}^q S_{i|i}^{(k)}(f) + S_{i|j}^{(k)}(f). \qquad (11)$$

The kth spectral component $S_{i|j}^{(k)}(f)$, $i,j = 1,2$, has an associated frequency related to the pole frequency, $f(k) = \arg\{z_k\}/2\pi$, and power related to the pole residuals, $P_{i|j}(k) = r_k$ for real poles and $P_{i|j}(k) = r_k + r_k^*$ for complex conjugate poles. It is then possible to achieve a decomposition for the DC from y_j to y_i normalizing the spectral components to the total spectrum as follows:

$$255 \qquad \gamma_{ij}^2(f) = \sum_{k=1}^{q} \gamma_{ij}^{2(k)}(f), \quad \gamma_{ij}^{2(k)}(f) \triangleq \frac{S_{i|j}^{(k)}(f)}{S_i(f)}. \tag{12}$$

Furthermore, causal contributions to the spectral power can be obtained by integrating each spectral component over the whole frequency axis. This allows to exploit (11) for decomposing the variance of the process y_i, λ_i^2, as

$$\lambda_i^2 = \frac{2}{f_s} \int_0^{f_s/2} S_i(f) df = \sum_{k=1}^{q} P_{i|i}(k) + P_{i|j}(k) = \sum_{k=1}^{q} P_i(k) \tag{13}$$

where $P_{i|i}(k) = \frac{2}{f_s} \int_0^{f_s/2} S_{i|i}^{(k)}(f) df$ is the part of the variance of y_i due to its own dynamics and relevant to k^{th} oscillation (pole), $P_{i|j}(k) = \frac{2}{f_s} \int_0^{f_s/2} S_{i|j}^{(k)}(f) df$ is the part of the variance of y_i due to y_j and relevant to the kth pole, and by summing these two contributions to the variance we get the part of the variance of y_i relevant to the k-th pole, i.e, $P_i(k) = P_{i|i}(k) + P_{i|j}(k)$. Using these partial variances, the PSSC relevant to the kth oscillation is obtained as a local causal measure of coupling from y_j to y_i:

$$270 \qquad \gamma_{i|j}^2(k) \triangleq \frac{P_{i|j}(k)}{P_i(k)}. \tag{14}$$

The PSSC ranges between 0 and 1, being equal to 0 when the power of the kth oscillation of y_i (i.e. the oscillation at frequency f_k) is totally due to its internal dynamics and equal to 1 when it is totally caused by the dynamics of y_j assessed at the same frequency f_k. Given that the frequency f_k is associated to a specific causal spectral profile, the corresponding PSSC value represents an objective measure of the causal power at that frequency, so that the total causal power in a specific frequency band f can be easily computed summing all PSSC values with frequency within that band. Using the same formalism, we also define a local non-causal measure of gain (local PSSG) from y_j to y_i related to the kth pole as

$$G_{ij}^{\alpha}(k) \triangleq \sqrt{\frac{P_i(k)}{P_j(k)}}. \tag{15}$$

The gain measure defined in (15) relates the whole variability of the output process y_i to that of the input process y_j without attempting to separate causal and non-causal contributions. To get a causal measure, we consider only the power of y_i causally due to y_j and related to the kth pole and define the local PSSG from y_j to y_i as:

$$G_{i|j}^{\gamma}(k) = \sqrt{\frac{P_{i|j}(k)}{P_j(k)}}. \tag{16}$$

290

Note that, while the spectral causality is an adimensional measure, the spectral gain is expressed in units of measurement of the output series divided by units of measurement of the input series.

2.3 Computation in cardiovascular variability analysis

To evaluate the new proposed local measures in comparison with the traditional global measures of both causal coupling and gain, the latter distinguishing also between causal and non-causal indices, we considered pairs of simultaneously observed beat-to-beat time series of SAP and RR, corresponding respectively to realizations of the processes y_1 and y_2. In the frequency domain analysis, the coupling and gain functions were evaluated within the LF band, ranging from $f_{inf}^{LF} = 0.04$ Hz to $f_{sup}^{LF} = 0.15$ Hz [30], in order to minimize the effects of non-baroreflex mechanisms on the assessed measures and especially to avoid the confounding effects of respiration on SAP and RR, which are primarily confined in the HF band [14–18,30]. Accordingly, after computing the spectrum of RR and SAP as well as their partial spectra and decomposition, the global measures of causal coupling (6), non-causal gain (4) and causal gain (7) were averaged in the LF band to get the following indexes ($i, j = 1,2, i \neq j$):

- Global causal coupling: $\gamma_{ji}^2(LF) \triangleq \frac{1}{f_{sup}^{LF} - f_{inf}^{LF}} \int_{f_{inf}^{LF}}^{f_{sup}^{LF}} \gamma_{ji}^2(f) \, df$ (17)

- Global non-causal gain: $G_{ji}^{\alpha}(LF) \triangleq \frac{1}{f_{sup}^{LF} - f_{inf}^{LF}} \int_{f_{inf}^{LF}}^{f_{sup}^{LF}} G_{ji}^{\alpha}(f) \, df$ (18)

- Global causal gain: $G_{ji}^{\gamma}(LF) \triangleq \frac{1}{f_{sup}^{LF} - f_{inf}^{LF}} \int_{f_{inf}^{LF}}^{f_{sup}^{LF}} G_{ji}^{\gamma}(f) \, df$.   (19)

On the other hand, local band-specific measures were obtained applying the equations for causal coupling (14), non-causal gain (15) and causal gain (16) after summing the power content of all the components with central frequency f_k within the LF range, *i.e.* computing ($i, j = 1,2, i \neq j$):
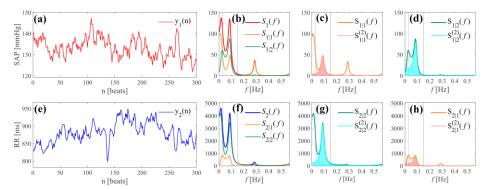
- Local causal coupling: $\gamma_{j|i}^2(k_{LF}) = \frac{\sum_{f_k \in LF} P_{j|i}(k)}{\sum_{f_k \in LF} P_j(k)}$ (20)

- Local non-causal gain: $G_{ji}^{\alpha}(k_{LF}) = \sqrt{\frac{\sum_{f_k \in LF} P_j(k)}{\sum_{f_k \in LF} P_i(k)}}$ (21)

- Local causal gain: $G_{j|i}^{\gamma}(k_{LF}) = \sqrt{\frac{\sum_{f_k \in LF} P_{j|i}(k)}{\sum_{f_k \in LF} P_i(k)}}$.   (22)

An example illustrating the causal spectral decomposition of the interactions between two processes is shown in Fig. 1 for representative SAP and RR time series. The derivation of the frequency measures of coupling and gain for the same time series is illustrated in Fig. 2.
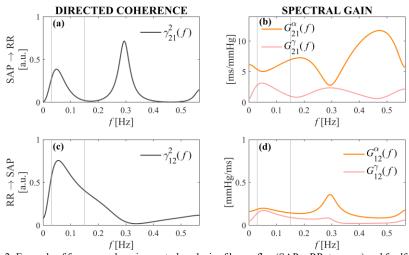
Figure 1. Example of causal spectral decomposition of the interactions between SAP and heart period (RR intervals). (a) and (e): SAP and RR time series, respectively, for a representative AMI subject in the resting supine position. (b): the power spectrum of SAP is given by $S_1(f)$ and is decomposed as the sum of a causal spectrum $[S_{1|2}(f)]$ and a non-causal spectrum $[S_{1|1}(f)]$; (c) and (d): the non-causal (c) and causal (d) spectra of SAP are in turn decomposed with the spectral decomposition method into contributions associated to specific oscillations of the time series, with those in the LF band (pole $k=2$) given by $S_{1|1}^{(2)}(f)$ (non-causal part, c) and $S_{1|2}^{(2)}(f)$ (causal part, d). (f): the power spectrum of RR is given by $S_2(f)$ and is decomposed as the sum of a causal spectrum $[S_{2|1}(f)]$ and a non-causal spectrum $[S_{2|2}(f)]$; (g) and (h): the non-causal (g) and causal (h) spectra of RR are in turn decomposed into contributions associated to specific oscillations, with those in the LF band given by $S_{2|2}^{(2)}(f)$ (non-causal part, g) and $S_{2|1}^{(2)}(f)$ (causal part, h). Local measures are computed as follows: the PSSC from SAP to RR in the LF band, $\gamma_{21}^2(k_{LF})$, is computed as the ratio between the power $P_{2|1}^{(2)}(LF)$ (pink area, (h)) and the total power $P_{2|1}^{(2)}(LF) + P_{2|2}^{(2)}(LF)$ (pink + cyan areas, (h) and (g)); the non-causal PSSG from SAP to RR in the LF band, $G_{21}^\alpha(k_{LF})$, is computed as the squared root of the ratio between the total power $P_{2|1}^{(2)}(LF) + P_{2|2}^{(2)}(LF)$ (pink + cyan areas, (h) and (g)) and the total power $P_{1|2}^{(2)}(LF) + P_{1|1}^{(2)}(LF)$ (cyan + pink areas, (d) and (c)); the causal PSSG from SAP to RR in the LF band, $G_{21}^\gamma(k_{LF})$, is computed as the squared root of the ratio between the power $P_{2|1}^{(2)}(LF)$ (pink area, (h)) and the total power $P_{1|2}^{(2)}(LF) + P_{1|1}^{(2)}(LF)$ (cyan + pink areas, (d) and (c)). The same procedure applies to the computation of the directed coherence and gain indexes from RR to SAP.

Figure 2. Example of frequency domain spectral analysis of baroreflex (SAP→RR, top row) and feedforward (RR→SAP, bottom row) interactions for a representative AMI subject in the resting supine position. (a) and

(c): directed coherence function, $\gamma_{ij}^2(f)$ (*i,j=1,2* and *i≠j*); (b) and (d): spectral profiles of the non-causal gain $G_{ij}^\alpha(f)$ and of the causal gain $G_{ij}^\gamma(f)$ (*i,j=1,2* and *i≠j*). These 'frequency-specific' measures were averaged in the low frequency band (vertical grey lines in each plot) to get global measures.

2.4 Experimental protocol and data analysis

The time series analyzed in this study are taken from an historical database already employed in previous works [7,31] for analyzing the effects of aging and myocardial infarction on heart rate variability and cardiovascular interactions. The study included 35 post-AMI patients (58.5 ± 10.2 yrs, 4 female), examined 10 ± 3 days after AMI, and two groups of healthy subjects, 19 young (25.0 ± 2.6 yrs, 9 female) and 12 old (63.1 ± 8.3 yrs, 9 female), all monitored in the resting supine position and in the 60° upright position reached after passive head-up tilt [7,31]. Young and old subjects were normotensive and without any known disease based on anamnesis and physical examination at the time of the study. Only patients with normal sinus rhythm, not taking antiarrhythmic drugs, and with preserved ventricular function and absence of myocardial ischemia, were chosen as the post-AMI patients among those included in a more complete database presented in [32]. All the analyzed time series consisted of sequences of 300 points fulfilling stationarity criteria [31,33].

Each pair of RR and SAP series were fitted by a bivariate AR model, after allowing instantaneous zero-lag effects in the direction from SAP to RR (i.e., setting $a_{21}(0) \neq 0$ and $a_{ij}(0) = 0$ as a constraint for model identification), to allow fast within-beat baroreflex influences in agreement with the adopted measurement convention. Model identification was performed via the vector least-squares approach, setting the model order *p* according to the multivariate version of the Akaike Information Criterion (AIC) [34]. In some cases, the use of the AIC led to negative power contributes and/or complex coupling and gain indices as a result of the residue theorem, which may have caused erroneous final results. This behavior is not unusual when carrying out spectral decomposition on cardiovascular time series because the AIC, which works fairly well with pure AR processes, has been reported to exhibit some limitations when analyzing biological signals, e.g. the loss of important spectral features of the underlying processes or the emergence of negative spectral components as a result of spectral decomposition [35]. The latter are typically ascribed to the splitting of the power associated to an oscillation in two or more poles, some of them bringing negative contribution. To circumvent this issue, all the obtained results were manually checked and, in case of negative power contributions, the model order was decreased iteratively from *p* to p-*k* (*k=1,2,...*) until a single component with positive power was detected.

After AR identification, estimation of the global and local measures of causal coupling and causal and non-causal gain were computed from the estimated model parameters, as described in the previous sections. Spectral analysis was performed assuming the series as uniformly sampled with the mean heart period $\langle RR \rangle$ taken as the sampling period T_s, so that the Nyquist frequency in each spectral representation was taken as $\frac{f_s}{2} = \frac{1}{2\langle RR \rangle}$.

As regards the statistical analysis, the distributions of the coherence and gain indices were tested for normality using the Anderson-Darling test [36,37]. Since the hypothesis

390 of normality was rejected for most of the distributions, and given the small sample size especially for young and old subjects, non-parametric tests were employed [38]. For any given group, the statistical significance of the difference between rest and tilt conditions was assessed using the Wilcoxon signed-rank test [39]. Afterwards, the statistical significance of the differences of the median of the distributions among
395 groups at a given physiological condition (rest or tilt) was assessed using the non-parametric Kruskal Wallis test [40]. When the null hypothesis that the data in each group comes from the same distribution was rejected, a pairwise comparison was carried out using the Dunn post-hoc test with Šidák correction for multiple comparisons (n=3) [41,42] to assess differences between group pairs (Young vs Old, Old vs AMI
400 and Young vs AMI) at a given condition (rest or tilt). Finally, to assess the statistical differences between global and local or causal vs non-causal indices given the group and the condition, the Wilcoxon signed rank test [39] was employed. All statistical tests were carried out with 5% significance level.

3. Results

405 In this section, the results of LF spectral decomposition and analysis are reported showing the distributions of the causal and non-causal indices described in Section 2, alongside with the outcomes of the statistical analyses carried out between different physiological conditions and between the various measures. The results in terms of causal coupling measures and of gain measures are depicted in Figures 3 and 4,
410 respectively.

In the baroreflex direction from SAP to RR (Fig. 3, top panels), both global and local measures of causal coupling were significantly higher during tilt than during rest for all groups, showing a clear response to postural stress of the DC along the baroreflex. Moreover, while the global values were significantly lower in Old and AMI subjects
415 compared with Young during both rest and tilt (Fig. 3a), the local index showed a significant decrease only in AMI compared with Young in both postural conditions (Fig. 3b).

As regards the gain measures in the same direction (Fig. 4, top panels), the non-causal indices decreased in Old compared to Young during postural stress, while they
420 did not elicit striking differences relevant to the AMI group (Fig. 4a,c). On the contrary, the causal gain indices (measured both globally and locally) detected a statistically significant decrease of the gain not only in Old, but also in AMI compared to Young, in both body positions (Fig. 4b,d). Moreover, the comparison between the two experimental conditions revealed that the gain index decreased significantly moving
425 from rest to tilt in all the three groups if computed using the non-causal methods (Fig. 4a,c), only in AMI patients using the causal global method (Fig. 4b), and in none of the groups using the causal local method (Fig. 4d).
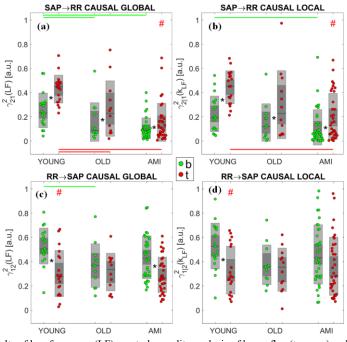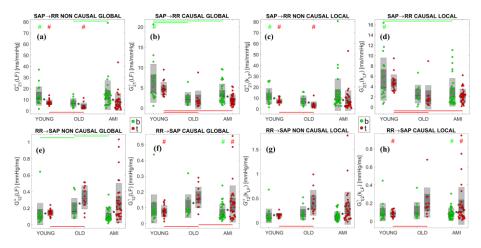
Figure 3. Results of low frequency (LF) spectral causality analysis of baroreflex (top row) and feedforward (bottom row) interactions based on the global and local directed (causal) coherence (respectively, $\gamma_{ij}^2(LF)$ and $\gamma_{ij}^2(k_{LF})$, where i,j=SAP, RR and $i \neq j$). Plots depict the distributions across subjects, shown as individual values and box-plot distributions, of the directed coherence from SAP to RR and from RR to SAP, computed in the supine (green) and upright (red) body positions. Statistically significant differences: *, rest vs. tilt; #, global vs. local; −, YOUNG vs. OLD, YOUNG vs. AMI or OLD vs. AMI.

Global and local measures of coupling and gain were also investigated in the feedforward direction, where mechanical effects are known to alter SAP variability according to changes in RR variability [16]. The local measure of causal coupling decreased significantly from rest to tilt in Young but not in Old and AMI (Fig. 3d). The corresponding global measure of feedforward coupling decreased with tilt also in the AMI patients, and was lower in Old than in Young in the supine position (Fig. 3c). As regards the gain from RR to SAP, the non-causal measures (both global and local) were significantly higher during orthostatic stress in all three groups (Fig. 4e,g), while the causal global measure increased significantly in Old and AMI (Fig. 4f) and the causal local measure increased significantly only in AMI (Fig. 4h).

Fig. 4 also illustrates that causal measures of gain are always lower than the corresponding non-causal ones, which is an obvious consequence of their mathematical formulation (i.e., the global causal gain (7) is obtained multiplying the global non-causal gain (4) by the DC, and the local causal gain (16) contains at the numerator a fraction of the power contained in the global non-causal gain (15)). Moreover, local measures tend to be lower in value than the corresponding global ones, being related to a specific oscillation in the LF band; the statistically significant differences in Fig. 4 are just a few, i.e. for Young (tilt and rest) and Old (tilt) in SAP→RR non causal index, for Young (rest) with regard to SAP→RR causal index and for Young and AMI (tilt) causal

index in RR→ SAP direction. Instead, comparing DC measures (Fig. 3), global and local indices resulted statistically different just for AMI tilt (SAP→RR direction) and for Young tilt (RR→SAP).

Figure 4. Distributions over subjects of the BRS computed in the LF band with the two different approaches (from left: non-causal and causal global measures, non-causal and causal local measures) along the two directions of interest (top: baroreflex direction from SAP to RR; bottom: feedforward direction from RR to SAP), in the rest (green) and tilt (red) phases of the testing protocol. Statistically significant differences: *, rest vs. tilt; #, global vs. local; −, YOUNG vs. OLD, YOUNG vs. AMI or OLD vs. AMI.

4. Discussion

Evaluation of the baroreflex gain is considered an important tool in clinical practice for diagnosis and prognosis in many cardiac diseases, including acute myocardial infarction [4–7,10,13]. A decreased baroreflex sensitivity has been observed in several pathological conditions as a marker of cardiovascular system impairment [7,10,13]. In this study, we propose a new method to assess the BRS in the frequency domain, investigating the usefulness of using local causal measures (*i.e.* 'pole-specific' measures) in place of already widely employed global approaches (*i.e.* 'frequency-specific' measures); the comparison is extended to non-baroreflex (feedforward) interactions to investigate the relevant underlying mechanisms.

Causal methods have been already proved in the literature as useful tools, typically more reliable than non-causal ones, for the quantitative assessment of cardiovascular regulatory mechanisms [10,20,43]. Moreover, preliminary results have shown that the frequency-averaging approaches commonly undertaken to obtain an individual value from a spectral function (e.g., the DC) for evaluating it within a specific band of interest (e.g., the LF band) may be inaccurate as they can incorporate spectral contributions originating from neighboring frequency ranges [25]. In the following, we compare more thoroughly causal vs non-causal (Sect. 4.1) and local vs global indices (Sect. 4.2) based on our results obtained on Young, Old and AMI patients monitored at rest and during head-up tilt. Then, assuming the suitability of causal local measures to characterize

feedback and feedforward cardiovascular interactions, in Sect. 4.3 we focus the discussion on the results obtained with such approach, both confirming expected physiological behaviors and suggesting novel interpretations for behaviors not established in the literature. Finally, in Sect. 4.4 we state the limitations of the proposed approach and envisage possible future studies.

4.1 Causal vs. non-causal assessment of cardiovascular interactions

In physiological conditions, RR and SAP normally reciprocally affect each other due to both the baroreflex regulatory feedback and the mechanisms of feedforward coupling (mainly of mechanical nature, such as the Windkessel and Frank-Starling effects) [21,43]. The presence of a closed-loop interaction between the heart period and the systolic arterial pressure highlighted by past works [2,21,43,44] suggests the importance to implement causality to assess cardiovascular interactions.

Our results confirm the findings already reported in the literature [10,20,43], highlighting the suitability of a causal method (γ index) versus a non-causal method (α index) for the frequency domain evaluation of BRS. Given the mathematical formulation of both indices (compare Eqs. (7) vs (4)), the non-causal measures are always higher than the causal ones (see also Fig. 4). This points out the unsuitability of non-causal measures to properly discriminate between the two directions of interaction in closed-loop bivariate processes. In the case of cardiovascular variability, this results in the inability of non-causal method to separate feedback and feedforward mechanisms, and in an overestimation of the BRS [10,13]. On the other hand, the closed-loop modeling of a causal method allows to separately evaluate feedback and feedforward pathways, quantifying their relative contribution to the overall cardiovascular regulation, thus extracting a more reasonable estimation of BRS [10].

The mixing between feedback and feedforward RR-SAP interactions can be also the reason why the non-causal measures of BRS detected a lower gain during postural stress not only in the AMI patients, but also in the Old and Young healthy subjects. The effect of the tilt maneuver on the power spectrum of HRV is widely known [45–48], as it is recognized that it evokes a greater effectiveness of the baroreflex that is mirrored by higher values of coupling between SAP and RR during postural stress; this effect was observed both in the present and in previous investigations [10,16,26]. Nevertheless, a decrease of the magnitude of the reflex, mirrored by the gain estimate, is more difficult to explain physiologically; in our work, the latter was observed only in the AMI patients using the global causal measure. Moreover, the causal measures of gain (both global and local) highlighted a significantly lower gain in the Old group, and especially in the AMI group, compared to the Young group. These decreased BRS values were observed in both the supine and upright position, documenting a reduced response of the baroreflex likely related to an impairment occurring with the coronary disease.

As regards the mechanical feedforward, the significant increase with head-up tilt observed for the non-causal measures of gain in all groups was found consistently for both causal measures only in the AMI patients. This result may be an indication of a physiological response to tilt that occurs as a consequence of the disease (as discussed

in Sect 4.3), and is observed in young healthy subjects only when non-causal methods are improperly used to assess the gain function.

4.2 Global vs. local assessment of cardiovascular interactions

From a methodological point of view, the operation of averaging spectral functions (like the DC or the gain) to get a global index within an assigned frequency band could lead to inaccurate evaluation of the index, because external broadband oscillations may convey information into the analyzed band. This aspect, that we have documented in a theoretical example in [25], is a major deal in cardiovascular variability analysis where VLF oscillations are often predominant and may thus have an impact on the evaluation of the DC or the BRS in the LF band of the spectrum, especially in heart disease patients [49,50]; a similar effect of spreading between adjacent bands may involve also the HRV oscillations located in the HF band and mainly due to respiration [14,30,45]. On the other hand, the method of spectral decomposition allows to focus more objectively on the spectral content within specific ranges, lastly resulting in DC and gain values (local measures) which are expected to reflect more accurately the underlying mechanisms of effectiveness and magnitude of a reflex with regard to the oscillations of physiological interest.

In the light of the methodological considerations above, we interpret the agreement often found between global and local measures as indicative of a limited impact of broadband VLF or HF spectral contributions into the analyzed LF band. This was the case, in the feedback direction from SAP to RR, for the significantly lower values of both causal coupling and gain observed in AMI compared to Young in both body positions and for the increase with tilt of the causal coupling in all groups, and, in the feedforward direction from RR to SAP, for the decrease in Young (but not in Old and AMI) of the causal coupling and the increase in AMI (but not in Young) of the causal gain observed moving from rest to tilt. These results, consistently found using both global and local causal measures, are interpreted as robust and are discussed physiologically in Sect. 4.3.

On the other hand, a disagreement between global and local measures of causal influence is likely indicating an effect of bands external to the LF on the global computation based on averaging. Such a disagreement was particularly evident for post-AMI patients along the baroreflex direction (SAP to RR) and was also found in terms of linear regression analysis (data not shown). In our results, the main occurrence of this disagreement is the detection in AMI of a significant causal gain decrease from SAP to RR observed moving from rest to tilt with the global method but not with the local method. This suggests that, in the analyzed post-infarction patients, the depressed BRS response to tilt suggested by global measures of gain is likely due to contributions to cardiovascular variability located in frequency bands other than the LF. This behavior is expected in response to tilt, as the sympathetic activation induced by the orthostatic stress is known to reduce the variability of RR in the VLF and especially HF bands and thus to isolate the power content in the LF band [48,51]. Moreover, the effect may be emphasized in AMI patients where confounding effects may arise also from the VLF band; in fact, the presence of important VLF rhythms has been put in relation to

the markedly impaired autonomic control of cardiovascular system, down-regulation of baroreceptor function and enhancement of chemosensitivity, especially in subjects presenting a more augmented sympathetic tone and attenuated baroreflex activity [49]. The other differences observed between the global and local approaches mostly concern comparisons involving the Old group; these may be explained also by the small size of this group (see Sect. 4.4).

4.3 Characterization of feedback and feedforward cardiovascular interactions via a local causal approach

As discussed in the previous subsections, the local causal method may be considered a methodologically more reasonable approach for assessing the coupling and gain related to specific oscillations of the two analyzed time series, as it is able to separately evaluate feedback and feedforward pathways and to avoid confounding spectral contributions from other frequency ranges. In the analyzed data, the local causal approach showed a tendency to detect less statistically significant differences in the comparisons between groups and conditions; as these seem to be more conceivable and with a more robust physiological meaning, we discuss them from a physiological viewpoint.

Compared to the young healthy controls, a significantly lower causal coupling along the baroreflex direction from SAP to RR was detected in post-AMI patients during each of the two analyzed experimental conditions; the difference with Young was not statistically significant in the Old group when the local method was adopted to measure the causal coupling. This result is in agreement with previous findings achieved on the same dataset using a causal synchronization method which highlighted an overall lower synchronization index and an increase of the number of subjects showing uncoupled RR and SAP dynamics [7]. Moreover, the post-AMI patients also showed significantly an impaired baroreflex gain compared to the young subjects, both at rest and during tilt. This result, that was observed also in Old during tilt, can be attributed to the higher sympathetic tone of these subjects and to an inability to respond to changes in cardiac output by further sympathetic activation [7], and can be related to the known reduction of heart rate variability typically occurring in elderly and AMI subjects [28,52,53].

When the response to head-up tilt was analyzed, we observed in all groups a significant increase of the causal coupling along the baroreflex pathway moving from the supine to the upright position. This finding is typically related to the sympathetic activation produced by the postural stress induced by tilt [54,55] which has already been widely observed in the literature [45,46,48,56]. Overall, it reflects the increased effectiveness of the baroreflex in response to an orthostatic maneuver. The fact that it was observed also in the post-AMI patients, together with the observation that none of the groups denoted significant variations of the local causal gain moving from rest to tilt, seems to suggest that the baroreflex response to postural stress is preserved, after myocardial infarction, in terms of increased effectiveness and unaltered sensitivity of the reflex assessed in the LF band. As discussed in Sect. 4.2, this finding is only detectable using a local causal measure of BRS, and therefore it provides an original interpretation of the autonomic response to tilt in AMI patients that supports the

usefulness of the gain measure proposed in this study. On the other hand, the statistically significant decrease of the global causal gain observed with tilt only in AMI patients points out a decreased BRS due to tilt, which agrees with previous findings indicating a reduced overall capability to cope with the postural challenge after AMI [7,28]. We hypothesize that the symptoms of orthostatic intolerance manifested after AMI are associated with fluctuations of RR and SAP, which are not confined within the LF band of the spectrum, and are therefore relevant to physiological mechanisms not involved in the generation of the Mayer waves [57].

Along the feedforward direction, a significant decrease of the causal coupling after head-up tilt was detected in Young subjects but not consistently in Old or post-AMI patients. In healthy subjects, a statistically significant decrease with tilt of the coupling from RR to SAP was reported using causal methods in the time domain [58], where it was investigated in terms of the cascade of interactions from RR to diastolic blood pressure (DBP) and then to SBP. Physiologically, this causal coupling is associated with the cardiac run-off, the Windkessel effect and the Frank-Starling law, according to which modifications of the heart period affect the end diastolic volume and then the strength of the systolic contraction [58,59]. The tilt-induced decrease of the effectiveness of the feedforward mechanism can be associated by the increased heart rate which limits the cardiac run-off and consequently the systolic contraction, but other mechanisms cannot be excluded as blood pressure variability is also due to variations in the sympathetic blood vessels control [43]. The lack of a consistent reduction with tilt of the feedforward coupling in Old and AMI patients could thus be associated to an impairment of these physiological mechanisms related to age and disease.

The feedforward gain was found to increase in Old and post-AMI patients after orthostatic stress. Since the occurrence of acute myocardial infarction is thought to be responsible of a significant stiffening of the cardiac muscle, and aging is associated with a stiffening of the vascular bed, these alterations might lead to an alteration of the mechanical effects, which allow heart period to drive SAP variability during head-up tilt. A role may be also played by the neural autonomic control, with a larger reduction of heart rate variability compared to SAP variability in AMI patients. The feedforward gain was found to significantly increase with the postural stress also in Old compared to Young subjects. The alteration of the capability of RR to drive SAP variability reported in Old people during tilt suggests that also aging can be responsible for a modification of feedforward mechanisms of mechanical nature that characterize the interactions from the heart period to the systolic arterial pressure. These results are in agreement with previous findings reported in [7] that highlighted an unbalanced RR-SAP regulation in old subjects with increased feedforward and decreased feedback mechanism.

4.4 Limitations and future studies

The present study has some limitations that should be taken into account. First of all, according to the study protocol [7], cardiovascular signals of the AMI group were recorded at predischarge time on patients in pharmacological washout. Only a small subgroup of very low-risk post-AMI patients able to support the suspension of β-

blocker treatment without appreciable risk and no taking of antiarrhythmic drugs was involved in the study. Therefore, the results of our study cannot be generalized to the general post-AMI population. Nonetheless, residual effects of the treatment with β-blockers may still be present in the AMI patients and thus affect the analyzed cardiovascular dynamics [31].

Other limitations are related to the small sample size of Young (19 subjects) and especially Old (12 subjects) groups, and to the fact that such groups are not homogeneous in the gender distribution (males are prevalent in AMI, females are prevalent in Old, while the gender is balanced in Young) [31].

Regardless of the type of the methodology used to assess causal coupling and gain, concerns as regards the computation of these values may arise from a number of factors that can complicate the estimation (e.g. choice of model order, noise effects, artifacts, and data filtering). In particular, a methodological limitation consists in the selection of the order of the parametric model used to fit the time series. Model order selection is an issue in real data analyses, where the true order is usually unknown. A correct model order assessment is rather difficult because the estimated order may not meet the desired specifications (in terms of spectral resolution when it is too low, or in terms of interpretability of highly variable spectral profiles when it is too high). In the present study, the use of the AIC [34] for model order selection led sometimes to spectral contributes of difficult interpretation or even negative power values after spectral decomposition. For this reason, the manual selection of the model order p could represent a possible workaround to avoid negative power contributes and to obtain a better spectral representation in LF band, still maintaining a tradeoff between good data resolution and reasonably low model complexity.

Future activities may also include further studies on larger groups of subjects, or on patients affected by different pathologies (e.g. hypertension [60,61] or atherosclerosis [62,63]). Moreover, an improvement of the automatic order selection algorithm to avoid negative power values or the application of other criteria (e.g. Bayesian Information Criterion) may be envisaged [64].

5.   Conclusion

This study emphasizes the importance of combining the novel method of spectral decomposition [24,65] and a causal approach to cross-spectral analysis [10,13] to investigate the coupling and gain mechanisms underlying the closed-loop cardiovascular regulation in healthy and diseased physiological states. Combining such approaches allows to quantify objectively, at specific well-defined frequencies, the causal contribution of SAP to RR along the baroreflex pathway and of RR to SAP along the mechanical feedforward. The application of the proposed method to cardiovascular time series of Young, Old and AMI subjects highlighted that causal local measures allow a reasonably more reliable assessment of BRS than traditional non-causal approaches, suggesting that aging and infarction generate impairment of BRS occurring at rest and when carrying out the orthostatic maneuver.

Our findings support the concept that the use of a spectral decomposition approach, as well as the implementation of causality in the study of interactions between heart

700 rate and arterial pressure, allows to mitigate the confounding effects of other variables operating at different frequencies and of reverse-side mechanisms and is thus essential to achieve a more accurate BRS assessment in physio-pathological states and different postural conditions.

CRediT authorship contribution statement

705 **Riccardo Pernice:** Methodology, Software, Visualization, Writing-Original draft preparation. **Laura Sparacino:** Software, Visualization, Writing-Original draft preparation. **Giandomenico Nollo**: Data curation. **Salvatore Stivala**: Writing-Reviewing and Editing**. Alessandro Busacca**: Writing- Reviewing and Editing**. Luca Faes:** Methodology, Formal analysis, Validation, Writing- Reviewing and Editing, 710 Supervision

Funding

715 ## References

[1]   R. Barbieri, G. Parati, J.P. Saul, Closed-versus open-loop assessment of heart rate baroreflex, IEEE Eng. Med. Biol. Mag. 20 (2001) 33–42.

[2]   G. Parati, P. Castiglioni, A. Faini, M. Di Rienzo, G. Mancia, R. Barbieri, J.P. Saul, Closed-Loop cardiovascular interactions and the baroreflex cardiac arm: 720 modulations over the 24 h and the effect of hypertension, Front. Physiol. 10 (2019) 477.

[3]   T. Zanotto, T.H. Mercer, M.L. van der Linden, J.P. Traynor, C.J. Petrie, A. Doyle, K. Chalmers, N. Allan, J. Price, H. Oun, Baroreflex function, haemodynamic responses to an orthostatic challenge, and falls in haemodialysis 725 patients, PLoS One. 13 (2018) e0208127.

[4]   M.T. La Rovere, G.D. Pinna, G. Raczak, Baroreflex sensitivity: measurement and clinical implications, Ann. Noninvasive Electrocardiol. 13 (2008) 191–

207.

[5]   T. Yasumasu, G.A. Reyes del Paso, K. Takahara, Y. Nakashima, Reduced baroreflex cardiac sensitivity predicts increased cognitive performance, Psychophysiology. 43 (2006) 41–45.

[6]   G.A. Reyes Del Paso, M.I. González, J.A. Hernández, S. Duschek, N. Gutierrez, Tonic blood pressure modulates the relationship between baroreceptor cardiac reflex sensitivity and cognitive performance, Psychophysiology. 46 (2009) 932–938.

[7]   G. Nollo, L. Faes, A. Porta, B. Pellegrini, F. Ravelli, M. Del Greco, M. Disertori, R. Antolini, Evidence of unbalanced regulatory mechanism of heart rate and systolic pressure after acute myocardial infarction, Am. J. Physiol. - Hear.   Circ.   Physiol.   283   (2002)   1200–1207. https://doi.org/10.1152/ajpheart.00882.2001.

[8]   G.M. De Ferrari, A. Sanzo, A. Bertoletti, G. Specchia, E. Vanoli, P.J. Schwartz, Baroreflex sensitivity predicts long-term cardiovascular mortality after myocardial infarction even in patients with preserved left ventricular function, J. Am. Coll. Cardiol. 50 (2007) 2285–2290.

[9]   T.G. Farrell, O. Odemuyiwa, Y. Bashir, T.R. Cripps, M. Malik, D.E. Ward, A.J. Camm, Prognostic value of baroreflex sensitivity testing after acute myocardial infarction., Heart. 67 (1992) 129–137.

[10] L. Faes, M. Masè, G. Nollo, K.H. Chon, J.P. Florian, Measuring postural-related changes of spontaneous baroreflex sensitivity after repeated long-duration diving: Frequency domain approaches, Auton. Neurosci. Basic Clin. 178 (2013) 96–102. https://doi.org/10.1016/j.autneu.2013.03.006.

[11] J. Krohova, L. Faes, B. Czippelova, R. Pernice, Z. Turianikova, R. Wiszt, N. Mazgutova, A. Busacca, M. Javorka, Vascular resistance arm of the baroreflex: Methodology and comparison with the cardiac chronotropic arm, J. Appl. Physiol.   128   (2020)   1310–1320. https://doi.org/10.1152/japplphysiol.00512.2019.

[12]   E.E. Benarroch, The arterial baroreflex: functional organization and involvement in neurologic disease, Neurology. 71 (2008) 1733–1738.

[13]   L. Sparacino, R. Pernice, G. Nollo, L. Faes, Causal and Non-Causal Frequency Domain Assessment of Spontaneous Baroreflex Sensitivity after Myocardial Infarction, in: 2020 11th Conf. Eur. Study Gr. Cardiovasc. Oscil., IEEE, 2020: pp. 1–2.

[14]   J. Krohova, L. Faes, B. Czippelova, Z. Turianikova, N. Mazgutova, R. Pernice, A. Busacca, D. Marinazzo, S. Stramaglia, M. Javorka, Multiscale Information Decomposition Dissects Control Mechanisms of Heart Rate Variability at Rest and During Physiological Stress, Entropy . 21 (2019). https://doi.org/10.3390/e21050526.

[15]   M. Javorka, J. Krohova, B. Czippelova, Z. Turianikova, N. Mazgutova, R. Wiszt, M. Ciljakova, D. Cernochova, R. Pernice, A. Busacca, L. Faes, Respiratory Sinus Arrhythmia Mechanisms in Young Obese Subjects, Front. Neurosci. 14 (2020) 204. https://doi.org/10.3389/fnins.2020.00204.

[16]   L. Faes, G. Nollo, A. Porta, Mechanisms of causal interaction between short-term RR interval and systolic arterial pressure oscillations during orthostatic challenge, J. Appl. Physiol. 114 (2013) 1657–1667.

[17]   F. Rahman, S. Pechnik, D. Gross, L. Sewell, D.S. Goldstein, Low frequency power of heart rate variability reflects baroreflex function, not cardiac sympathetic innervation, Clin. Auton. Res. 21 (2011) 133–141.

[18]   D.S. Goldstein, O. Bentho, M. Park, Y. Sharabi, Low-frequency power of heart rate variability is not a measure of cardiac sympathetic tone but may be a measure of modulation of cardiac autonomic outflows by baroreflexes, Exp. Physiol. 96 (2011) 1255–1261.

[19]   A. Porta, R. Furlan, O. Rimoldi, M. Pagani, A. Malliani, P. Van De Borne, Quantifying the strength of the linear causal coupling in closed loop interacting cardiovascular variability signals, Biol. Cybern. 86 (2002) 241–251.

[20]   L. Faes, A. Porta, R. Cucino, S. Cerutti, R. Antolini, G. Nollo, Causal transfer

function analysis to describe closed loop interactions between cardiovascular and cardiorespiratory variability signals, Biol. Cybern. 90 (2004) 390–399.

[21]   G. Nollo, L. Faes, A. Porta, R. Antolini, F. Ravelli, Exploring directionality in spontaneous heart period and systolic pressure variability interactions in humans: implications in the evaluation of baroreflex gain, Am. J. Physiol. Circ. Physiol.   288   (2005)   H1777–H1785. https://doi.org/10.1152/ajpheart.00594.2004.

[22]   L. Faes, S. Erla, A. Porta, G. Nollo, A framework for assessing frequency domain causality in physiological time series with instantaneous effects, Philos. Trans. R. Soc. A Math. Phys. Eng. Sci. 371 (2013) 20110618.

[23]   M. Pagani, V. Somers, R. Furlan, S. Dell'Orto, J. Conway, G. Baselli, S. Cerutti, P. Sleight, A. Malliani, Changes in autonomic regulation induced by physical training in mild hypertension., Hypertension. 12 (1988) 600–610.

[24]   G. Baselli, A. Porta, O. Rimoldi, M. Pagani, S. Cerutti, Spectral decomposition in multichannel recordings based on multivariate parametric identification, IEEE   Trans.   Biomed.   Eng.   44   (1997)   1092–1101. https://doi.org/10.1109/10.641336.

[25]   L. Faes, J. Krohova, R. Pernice, A. Busacca, M. Javorka, A new Frequency Domain Measure of Causality based on Partial Spectral Decomposition of Autoregressive Processes and its Application to Cardiovascular Interactions*, in: 2019 41st Annu. Int. Conf. IEEE Eng. Med. Biol. Soc., 2019: pp. 4258–4261. https://doi.org/10.1109/EMBC.2019.8857312.

[26]   M. Di Rienzo, G. Parati, P. Castiglioni, R. Tordi, G. Mancia, A. Pedotti, Baroreflex effectiveness index: an additional measure of baroreflex control of heart rate in daily life, Am. J. Physiol. Integr. Comp. Physiol. 280 (2001) R744–R751.

[27]   B.E. Westerhof, J. Gisolf, J.M. Karemaker, K.H. Wesseling, N.H. Secher, J.J. Van Lieshout, Time course analysis of baroreflex sensitivity during postural stress, Am. J. Physiol. Circ. Physiol. 291 (2006) H2864–H2874.

815   [28]   F. Lombardi, G. Sandrone, S. Pernpruner, R. Sala, M. Garimoldi, S. Cerutti, G. Baselli, M. Pagani, A. Malliani, Heart rate variability as an index of sympathovagal interaction after acute myocardial infarction, Am. J. Cardiol. 60 (1987) 1239–1245.

[29]   L. Faes, S. Erla, G. Nollo, Measuring connectivity in linear multivariate processes: definitions, interpretation, and practical analysis, Comput. Math. Methods Med. 2012 (2012).

[30]   F. Shaffer, J.P. Ginsberg, An Overview of Heart Rate Variability Metrics and Norms, Front. Public Heal. 5 (2017) 258. https://doi.org/10.3389/fpubh.2017.00258.

825   [31]   L. Faes, M. Gómez-Extremera, R. Pernice, P. Carpena, G. Nollo, A. Porta, P. Bernaola-Galván, Comparison of methods for the assessment of nonlinearity in short-term heart rate variability under different physiopathological states, Chaos An Interdiscip. J. Nonlinear Sci. 29 (2019) 123114. https://doi.org/10.1063/1.5115506.

830   [32]   G. Nollo, M. Del Greco, M. Disertori, E. Santoro, A. Pietro Maggioni, G. Pietro Sanna, G.-3 A.S. Investigators, Absence of slowest oscillations in short term heart rate variability of post-myocardial infarction patients. GISSI-3 arrhythmias substudy, Auton. Neurosci. 90 (2001) 127–131.

[33]   W. Xiong, L. Faes, P.C. Ivanov, Entropy measures, entropy estimators, and their performance in quantifying complex dynamics: Effects of artifacts, nonstationarity, and long-range correlations, Phys. Rev. E. 95 (2017) 62114. https://doi.org/10.1103/PhysRevE.95.062114.

[34]   H. Akaike, A new look at the statistical model identification, IEEE Trans. Automat. Contr. 19 (1974) 716–723.

840   [35]   G.D. Pinna, R. Maestri, A. Di Cesare, Application of time series spectral analysis theory: analysis of cardiovascular variability signals, Med. Biol. Eng. Comput. 34 (1996) 142–148.

[36]   T.W. Anderson, D.A. Darling, Asymptotic theory of certain" goodness of fit"

criteria based on stochastic processes, Ann. Math. Stat. 23 (1952) 193–212.

845 [37] B.W. Yap, C.H. Sim, Comparisons of various types of normality tests, J. Stat. Comput. Simul. 81 (2011) 2141–2155.

[38] A.K. Dwivedi, I. Mallawaarachchi, L.A. Alvarado, Analysis of small sample size studies using nonparametric bootstrap test with pooled resampling method, Stat. Med. 36 (2017) 2187–2205.

850 [39] J.D. Gibbons, S. Chakraborti, Nonparametric Statistical Inference: Revised and Expanded, CRC press, 2014.

[40] J.H. McDonald, Handbook of biological statistics, 2009.

[41] S.S. Sawilowsky, Real data analysis, IAP, 2007.

[42] Z. Šidák, Rectangular confidence regions for the means of multivariate normal
855 distributions, J. Am. Stat. Assoc. 62 (1967) 626–633.

[43] M. Javorka, B. Czippelova, Z. Turianikova, Z. Lazarova, I. Tonhajzerova, L. Faes, Causal analysis of short-term cardiovascular variability: state-dependent contribution of feedback and feedforward mechanisms, Med. Biol. Eng. Comput. 55 (2017) 179–190.

860 [44] A. Porta, G. Baselli, O. Rimoldi, A. Malliani, M. Pagani, Assessing baroreflex gain from spontaneous variability in conscious dogs: role of causality and respiration, Am. J. Physiol. Circ. Physiol. 279 (2000) H2558–H2567.

[45] R. Pernice, M. Javorka, J. Krohova, B. Czippelova, Z. Turianikova, A. Busacca, L. Faes, Reliability of Short-Term Heart Rate Variability Indexes Assessed
865 through Photoplethysmography, in: 2018 40th Annu. Int. Conf. IEEE Eng. Med. Biol. Soc., 2018: pp. 5610–5613. https://doi.org/10.1109/EMBC.2018.8513634.

[46] R. Pernice, M. Javorka, J. Krohova, B. Czippelova, Z. Turianikova, A. Busacca, L. Faes, Comparison of short-term heart rate variability indexes evaluated
870 through electrocardiographic and continuous blood pressure monitoring, Med. Biol. Eng. Comput. 57 (2019) 1247–1263. https://doi.org/10.1007/s11517-019-

01957-4.

[47] A. Porta, E. Tobaldini, S. Guzzetti, R. Furlan, N. Montano, T. Gnecchi-Ruscone, Assessment of cardiac autonomic modulation during graded head-up tilt by symbolic analysis of heart rate variability, Am. J. Physiol. Circ. Physiol. 293 (2007) H702–H708. https://doi.org/10.1152/ajpheart.00006.2007.

[48] N. Montano, T.G. Ruscone, A. Porta, F. Lombardi, M. Pagani, A. Malliani, Power spectrum analysis of heart rate variability to assess the changes in sympathovagal balance during graded orthostatic tilt., Circulation. 90 (1994) 1826–1831.

[49] P. Ponikowski, T.P. Chua, A.A. Amadi, M. Piepoli, D. Harrington, M. Volterrani, R. Colombo, G. Mazzuero, A. Giordano, A.J.S. Coats, Detection and significance of a discrete very low frequency rhythm in RR interval variability in chronic congestive heart failure, Am. J. Cardiol. 77 (1996) 1320–1326.

[50] J.T. Bigger Jr, J.L. Fleiss, R.C. Steinman, L.M. Rolnitzky, R.E. Kleiger, J.N. Rottman, Frequency domain measures of heart period variability and mortality after myocardial infarction., Circulation. 85 (1992) 164–171.

[51] C. Miwa, Y. Sugiyama, T. Mano, T. Matsukawa, S. Iwase, T. Watanabe, F. Kobayashi, Effects of aging on cardiovascular responses to gravity-related fluid shift in humans, Journals Gerontol. Ser. A Biol. Sci. Med. Sci. 55 (2000) M329–M335.

[52] R.E. Kleiger, J.P. Miller, J.T. Bigger Jr, A.J. Moss, Decreased heart rate variability and its association with increased mortality after acute myocardial infarction, Am. J. Cardiol. 59 (1987) 256–262.

[53] H. Tsuji, F.J. Venditti Jr, E.S. Manders, J.C. Evans, M.G. Larson, C.L. Feldman, D. Levy, Reduced heart rate variability and mortality risk in an elderly cohort. The Framingham Heart Study., Circulation. 90 (1994) 878–883.

[54] D.D. O'leary, D.S. Kimmerly, A.D. Cechetto, J.K. Shoemaker, Differential effect of head-up tilt on cardiovagal and sympathetic baroreflex sensitivity in

humans, Exp. Physiol. 88 (2003) 769–774.

[55]   W.H. Cooke, J.B. Hoag, A.A. Crossman, T.A. Kuusela, K.U.O. Tahvanainen, D.L. Eckberg, Human responses to upright tilt: a window on central autonomic integration, J. Physiol. 517 (1999) 617–628.

[56]   A. Porta, T. Gnecchi-Ruscone, E. Tobaldini, S. Guzzetti, R. Furlan, N. Montano, Progressive decrease of heart period variability entropy-based complexity during graded head-up tilt, J. Appl. Physiol. 103 (2007) 1143–1149. https://doi.org/10.1152/japplphysiol.00293.2007.

[57]   M.A. Cohen, J.A. Taylor, Short-term cardiovascular oscillations in man: measuring and modelling the physiologies, J. Physiol. 542 (2002) 669–683. https://doi.org/10.1113/jphysiol.2002.017483.

[58]   M. Javorka, J. Krohova, B. Czippelova, Z. Turianikova, Z. Lazarova, K. Javorka, L. Faes, Basic cardiovascular variability signals: mutual directed interactions explored in the information domain, Physiol. Meas. 38 (2017) 877–894. https://doi.org/10.1088/1361-6579/aa5b77.

[59]   N. Westerhof, J.-W. Lankhaar, B.E. Westerhof, The arterial windkessel, Med. Biol. Eng. Comput. 47 (2009) 131–141.

[60]   G. Grassi, F.Q. Trevano, G. Seravalle, F. Scopelliti, G. Mancia, Baroreflex function in hypertension: consequences for antihypertensive therapy, Prog. Cardiovasc. Dis. 48 (2006) 407–415.

[61]   A. Berdeaux, J.F. Giudicelli, Antihypertensive drugs and baroreceptor reflex control of heart rate and blood pressure, Fundam. Clin. Pharmacol. 1 (1987) 257–282.

[62]   N. Nasr, A. Pavy-Le Traon, V. Larrue, Baroreflex sensitivity is impaired in bilateral carotid atherosclerosis, Stroke. 36 (2005) 1891–1895.

[63]   S. Simula, T. Laitinen, E. Vanninen, P. Pajunen, M. Syvänne, A. Hedman, J. Hartikainen, Baroreflex sensitivity in asymptomatic coronary atherosclerosis, Clin. Physiol. Funct. Imaging. 33 (2013) 70–74.

[64]   A.A. Neath, J.E. Cavanaugh, The Bayesian information criterion: background, derivation, and applications, Wiley Interdiscip. Rev. Comput. Stat. 4 (2012) 199–203.

[65]   L.H. Zetterberg, Estimation of parameters for a linear difference equation with application to EEG analysis, Math. Biosci. 5 (1969) 227–275. https://doi.org/https://doi.org/10.1016/0025-5564(69)90044-3.

930

935